Wheat *EARLY FLOWERING3* is a dawn-expressed circadian oscillator component that regulates heading date

Lukas Wittern[1¶], Gareth Steed[2¶], Laura J. Taylor[2], Keith Gardner[3], Andy Greenland[3], Matthew A. Hannah[1], Alex A. R. Webb[2]*

[1]BASF, BBCC – Innovation Center Gent, Technologiepark-Zwijnaarde, Gent, Belgium

[2]Department of Plant Sciences, University of Cambridge, Downing Street, Cambridge, CB2 3EA, UK

[3]NIAB, Huntingdon Road, Cambridge, UK

*Corresponding author

Email: aarw2@cam.ac.uk (AARW)

¶These authors contributed equally to this work

Funding LW, GS, and LJT were supported by BBSRC studentships BB/K011790/1, BB/M015416/1 and BB/M011194/1 awarded to MAH and AARW, GS is supported by UKRI BBSRC grant BB/S006370/1 awarded to AARW.

Abstract

Optimising the seasonal control of flowering in the major crops is an important component of breeding to match crop adaptation to the target environment. Using an eight parent Multiparent Advanced Generation Inter-Cross (MAGIC) population we investigated the contribution of variation at circadian clock-associated genes to the regulation of heading date (flowering) in UK and European winter wheat varieties. We identified homoeologues of *EARLY FLOWERING* 3 (*ELF3*) as candidate genes for the *Earliness per se* (*Eps*) *D1* and *B1 loci* in field conditions. We confirmed that a SNP within the coding region of *TaELF3-B1* is the likely causal polymorphism underlying the *Eps-B1 locus.* We also identified that a reported deletion at the *Eps-D1 locus* encompassing *TaELF3-D1,* is in fact a novel allele that lies within an introgression region that contains an inversion relative to the Chinese Spring D genome. Our findings that *ELF3* might be associated with the regulation of heading date prompted us to investigate whether *ELF3* is a circadian oscillator gene in wheat, as it is in Arabidopsis. Using *T. turgidum cv. Kronos* carrying loss of function alleles for both copies of *TtELF3* we found that circadian rhythms were severely disrupted. Furthermore, in *T. aestivum*, we found that loss of functional *LUX ARRHYTHMO* (*LUX*), an orthologue of the protein partner of ELF3 in Arabidopsis, also severely disrupted circadian rhythms. Whilst these data suggest a function for both *ELF3* and *LUX* in the wheat circadian oscillator, that oscillator might be structured differently to that of Arabidopsis because wheat *ELF3* and *LUX* transcripts are maximal at the end of the night and day respectively, rather than co-expressed at dusk as they are in Arabidopsis. We conclude that there is sufficient allelic diversity within the three wheat *ELF3* homoeologues for selection to delay or advance heading, and that this can be achieved without pleiotropic deleterious alterations to circadian rhythms.

Introduction

Circadian clocks are endogenous timing mechanisms with a near 24 hour period that sequence biological events, provide anticipation of environmental rhythms and permit measurement of daylength to regulate seasonal adjustments (1). Plant breeders have indirectly selected for variation at circadian-associated *loci* in many of the world's major crops when breeding to increase yield and improve crop performance by adapting genotypes to the local environment (2). Here we investigated whether variation at circadian associated *loci* contributes to wheat yield traits in the field using a Multiparent Advanced Generation Inter-Cross (MAGIC) mapping population (3). Wheat is a major crop, providing approximately 20% of the dietary calories and protein for the world's population (4). Since the green revolution wheat yields have continued to increase but with the world's population estimated to reach 9.6 billion in 2050 (5) it is likely that demand will outpace predicted yield increases (4). Identification of novel genetic variation contributing to yield is critical to increasing the rate of yield gains in wheat.

Understanding of the nature of circadian oscillators in the plant Kingdom is based primarily on investigation of Arabidopsis. In that model, the circadian oscillator contains a series of interlocking transcriptional feedback loops. The circadian oscillator cycle can be considered to start at dawn when expression of the transcriptional repressors *CIRCADIAN CLOCK ASSOCIATED 1* (*CCA1*) and *LATE ELONGATED HYPOCOTYL* (*LHY*) peaks, followed sequentially by peaks of expression of *PSEUDO REPSONSE REGULATOR 9* (*PRR9*), *PRR7, PRR5, PRR3* and finally *PRR1* (also known as *TIMING OF CAB EXPRESSION 1* (*TOC1*)) at dusk (6). PRR9 and PRR7 repress the expression of *CCA1* and *LHY* which releases repression of evening

phased genes including, *TOC1, GIGANTEA* (*GI*)*, EARLY FLOWERING 3* (*ELF3*)*, ELF4* and *LUX ARRHYTHMO* (*LUX*) (6). LUX is a MYB-like transcription factor which associates with ELF3 and ELF4 to form the tripartite evening complex (EC), which represses expression of *GI, TOC1, PRR7, PRR9* and *LUX* (7–9). Mutation of any of the three EC components causes arrhythmia of the Arabidopsis circadian oscillator in continuous light and temperature conditions (10).

Orthologues of *ELF3* underlie *loci* regulating heading date in multiple crops, including barley *early maturity8* (*eam8*) (11), rice *heading date17* (*Hd17*) (12), *Earliness per se* (*Eps*)-A^m*1* in *T. monococcum* and *Eps-D1* in *T. aestivum* (13). In hexaploid wheat, the magnitude of the *Eps-D1* effect on heading date increases with decreasing temperature (14). An orthologue of *GIGANTEA* (*GI*) is linked to susceptibility to spot blotch attack (15) and orthologues of *TOC1* are associated with heading date, plant height and thousand grain weight (16). An orthologue of *LUX* is a candidate for *Eps-3*A^m in *T. monococcum* (17) and *HvLUX* is a candidate gene for *eam10* in barley (18). Furthermore, the *Photoperiod-1* (*Ppd-1*) genes, which contribute to photoperiodic regulation of ear emergence, are orthologues of Arabidopsis *PRRs* (19–22).

We used the allelic diversity of a wheat MAGIC population to investigate the role of circadian clock genes in regulating yield component traits in the field. The founder varieties for the MAGIC population used in this study (Alchemy, Brompton, Claire, Hereward, Rialto, Robigus, Soissons and Xi-19) are representative of UK and European winter wheat varieties, capturing >80% of the polymorphism found across UK wheat varieties from the last 70 years (23). Our data suggest that breeding for modified *ELF3* function can affect the regulation of flowering time but potentially

without compromising yield through disrupted circadian oscillations, due to the separable contributions of *ELF3* homoeologues to flowering and circadian rhythms.

Results

Segregation of the *Eps-B1* and *Eps-D1* loci underlie QTL for heading date in a UK wheat MAGIC population

We obtained a set of replicated trial data for 784 recombinant inbred lines (RILs) for the NIAB Elite MAGIC population from the 2012/2013 and 2013/2014 growing seasons at the NIAB experimental farms in Cambridge, UK. Growth stage 55 (GS55, equivalent to heading date) (24) was chosen for analysis and QTL mapping to enable comparisons with previous studies (25). In both 2013 and 2014, Soissons, which contains the *Ppd-D1a* allele (photoperiod insensitive), reached GS55 6-8 days earlier than any of the other MAGIC parents, which contain the *Ppd-D1b* allele (photoperiod sensitive) (Fig 1). Flowering time of the other MAGIC parents varied over 5.5 days in 2013 and 7 days in 2014.

We performed QTL analysis using MPWGAIM (26) for GS55 phenotypes in both years and tested whether any circadian clock genes colocate with the identified QTLs. We found that four circadian gene orthologues (*TaELF3-B1, TaELF3-D1, Ppd-1, TaZTL-7A*) fell within 0.20, 0.27, 0.58 and 4.31 Mb respectively of one of the QTL flanking markers (Table 1). The absence of significant heading date QTLs linked to vernalisation genes such as *VRN1* confirmed that complete vernalisation had occurred, ensuring that observed variations in heading date were true *Earliness per-*

se (*Eps*) effects rather than a variation in the vernalisation requirements between the MAGIC parents (21,27).

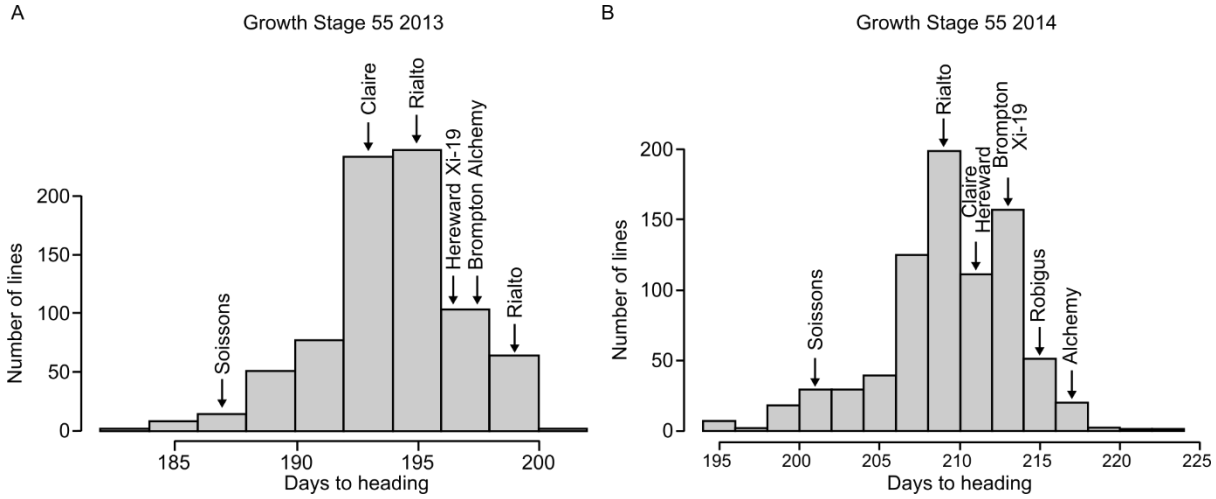

Fig 1. **Variation in time to reach GS55 across a UK wheat MAGIC population**.

Time in days for individual MAGIC RILs (recombinant inbred lines) to reach GS55 for the (A) 2012/2013 growing season and (B) 2013/2014 growing season. The number of days after sowing to reach GS55 for the eight MAGIC parents is indicated by arrows.

A QTL on the distal end of chromosome 1B, delineated by the markers Ra_c109187_371 and RAC875_c37075_283, mapped closely to the physical position of *TaELF3-B1* (TraesCS1B02G477400) (Table 1). The 1B locus also had a homoeologous QTL on chromosome 1D delineated by the markers Kukri_c29687_369 and Kukri_rep_c69829_307 identifying *TaELF3-D1* (TraesCS1D02G451200) as a candidate gene (Table 1, Fig 2A). These QTLs co-locate with the previously described heading data QTLs *Eps-B1* and *Eps-D1* (25). In our data *Eps-B1* had a significant effect in both years, explaining 3.4% of genetic variance in GS55 in 2013 and 2% in 2014 (Table 1). *Eps-D1* only had a significant effect (–log10(p) = 2.32) in 2014, accounting for 4.1% of genetic variance in GS55 in that year (Table 1). The *Eps-B1*

and *Eps-D1 loci* were chosen for further in-depth analysis because of their proximity to *ELF3* homoeologues.

Table 1: **Summary of circadian clock associated QTLs and their mapping positions.** Output from univariate QTL model for the NIAB 2013 and 2014 GS55 data. Gene (Mb) refers to the BLAST hit starting coordinate of the genes cDNA against the IWGSCRefSeqv1.1. Dist (cM) refers to the markers genetic mapping distance in centiMorgan. Dist (Mb) refers to the BLAST hit starting coordinate of the marker sequence against the IWGSCRefSeqv1.1 LOGP is –log10(p). % var is the percentage of genetic variance explained.

Circadian clock gene	Gene (Mb)	Chr	L. Marker	dist (cM)	dist(Mb)	R. Marker	dist (cM)	dist(Mb)	Year	LOGP	% var
TaELF3	685,646,575	1B	Ra_c109187_371	296.34	685,741,261	RAC875_c37075_283	297	687,715,336	2013	4.48	3.4
		1B	Ra_c109187_371	296.34	685,741,261	RAC875_c37075_284	297	687,715,336	2014	3.2	2
TaELF3	493,485,612	1D	Kukri_c29687_369	100.95	493,212,138	Kukri_rep_c69829_307	101.95	488,577,079	2014	2.32	4.1
Ppd-1	33,952,591	2D	Kukri_c27309_590	48.57	31,806,310	BS00064538_51	56.64	33,370,535	2013	20.04	17.2
		2D	Kukri_c27309_590	48.57	31,806,310	BS00064538_51	56.64	33,370,535	2014	43.92	30.2
TaZTL	625,638,942	7A	Kukri_c6676_172	207.62	610,934,248	Ku_c2990_1939	208.12	621,322,194	2013	2.87	2.6

TaELF3-B1 is a candidate gene for the *Eps-B1* QTL

At the 1B QTL, the alleles derived from the MAGIC parents Soissons, Alchemy, Robigus and Claire caused a relative reduction in the time to GS55, indicated by the negative sign of the QTL, whilst alleles from Rialto, Hereward, Xi-19 and Brompton caused a delay to GS55, indicated by the positive sign of the QTL (S1 Table). The interval between the markers Ra_c109187_371 (296.34cM / 685.7Mb) and RAC875_c37075_283 (297.00cM / 687.7Mb) is 0.66cM, corresponding to a physical length of ca. 2 Mb (Fig 2A). Recombination within the interval occurred in the line 6464 (MEL 209-5B), with the haplotype changing from Soissons at Ra_c109187_371 to

Robigus at RAC875_c37075_283. As both Soissons and Robigus belong to the same haplogroup it was not possible to determine which of the flanking markers segregated with the observed phenotypes.

The current IWGSCv1.1 gene annotation suggests there are 26 high confidence gene models within the interval of Ra_c109187_371 and RAC875_c37075_283. Based on current gene annotation and orthology to cloned rice genes (28) there are no novel candidates for the *Eps-B1* locus except those described previously (13,29,30). Compared to the *T. monococcum* physical map of the *Eps-A^{m}1* region (30) *TmADK* (similar to rice putative kinase *ADK1)* and *TmCK1-like* (*CASEIN KINASE I ISOFORM DELTA-LIKE)* are not syntenic and the locus containing *TaELF3*, *TaGRIK1-like* (*GEMINIVIRUS REP INTERACTING KINASE 1 LIKE*) and *TaPWWP1* (*PWWP domain-containing protein*) is inverted (Fig 2A). Nineteen genes had homoeologues on the syntenic 1D chromosome (Fig 2A).

Sanger sequencing of the *TaELF3-B1* gene in Soissons (S1 File) together with publicly available RNA-seq data for Alchemy, Hereward, Soissons and Xi-19 (31), the Claire and Robigus reference sequences (32) and the Rialto coding sequence (13) indicated that a SNP within exon 4 at position chr1B:685645813 is the only detected polymorphic SNP in the *TaELF3-B1* coding sequence in the MAGIC population. The SNP (Adenine at position 2020 of CDS to Guanine; A2020G) causes a predicted deleterious amino acid substitution from the ancestral serine to a glycine residue at position 674 of the predicted primary amino acid sequence (Ser674Gly; SIFT 0.01) (Fig 2B). A KASP marker was designed for this SNP and used to genotype the MAGIC population. The KASP marker mapped to the same genetic position as Ra_c109187_371 thus confirming that *TaELF3-B1* is part of the 1B GS55 QTL.

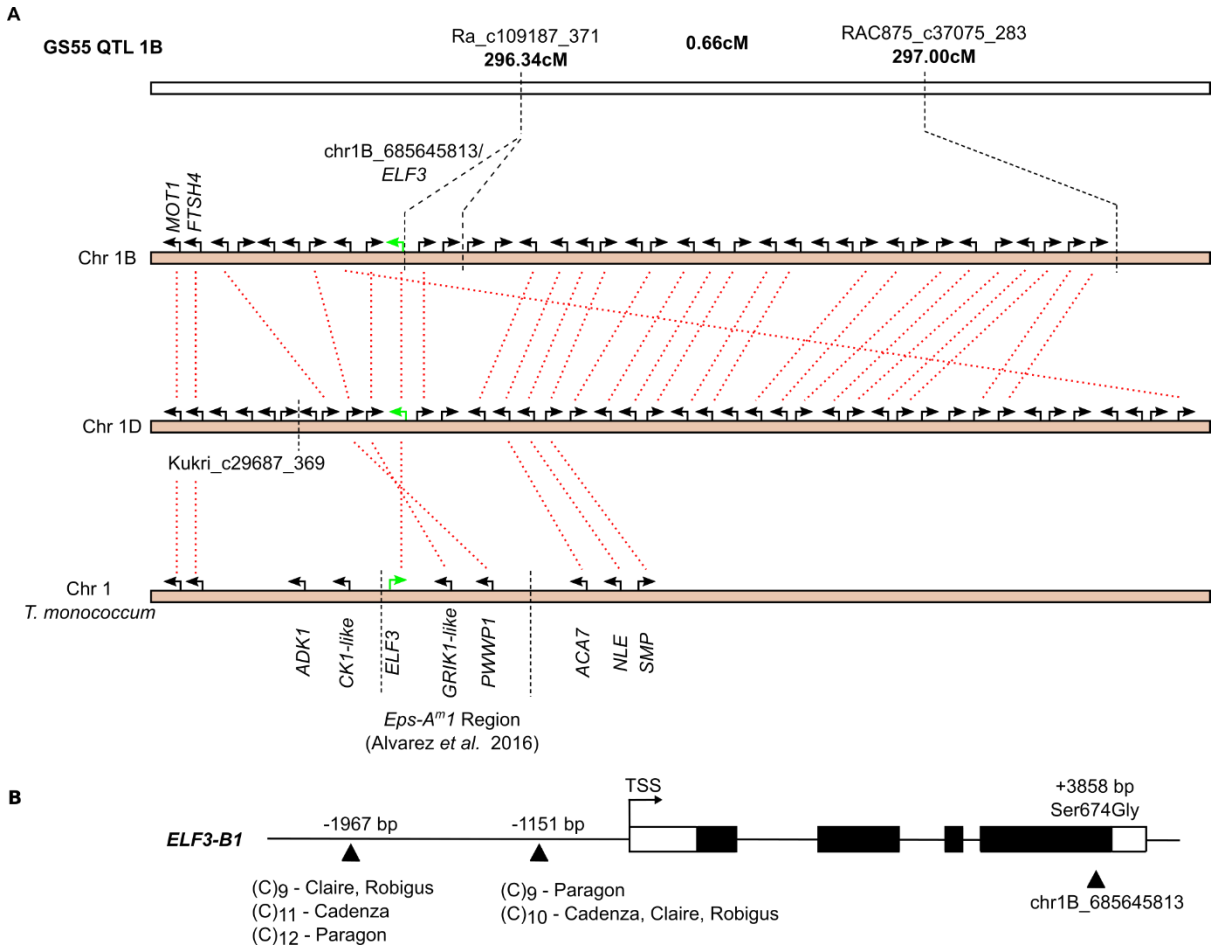

Fig 2. ***ELF3* is a candidate gene for *Eps-B1*.**

(A) Syntenic relationships of the *Eps-B1* QTL to the *Eps-D1* QTL and the *T. monococcum Eps-A^{m}1* QTL. *ELF3* highlighted in green. (B) *TaELF3-B1* gene model with exons represented by filled rectangles, UTR's as white rectangles. The two promoter cytosine repeat polymorphisms with location relative to the transcription start site (TSS) are indicated with the cytosine (C) repeat number for Claire, Robigus, Cadenza and Paragon. The Ser674Gly SNP is situated within exon 4 of *ELF3-B1.*

To confirm that the KASP marker amplifies the right haplotypes, we compared the marker calls to the predicted mean parental effects of the haplotypes between RAC875_c37075_283 (Hereward, Rialto, Soissons, Xi-19 vs. rest) and Ra_c109187_371 (Soissons minority parent). The marker calls corresponded with the predicted parental effects with the serine residue at position 674 associated with early

heading and the predicted glycine residue at position 674 associated with late heading (Fig 3).

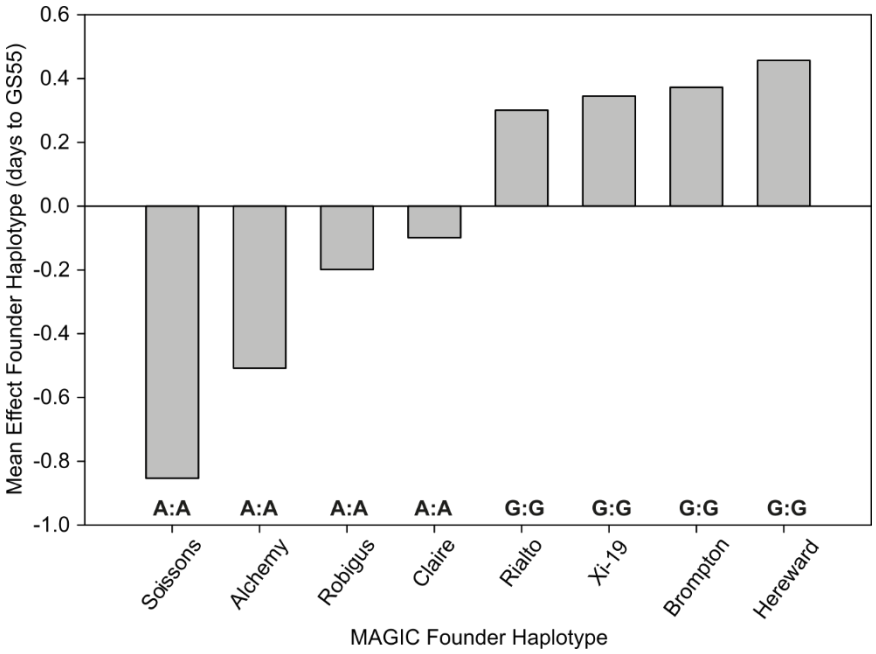

Fig 3. The Ser674Gly SNP is a candidate for the causal *Eps-B1* SNP.

KASP Genotype association with MAGIC founder haplotype effects at the *Eps-B1* locus. Founder haplotype effects are calculated as the mean of the 2013 and 2014 founder effect. Genotype of A|A corresponds to homozygous for adenine, encoding the ancestral Serine, whilst G|G corresponds to homozygous guanine encoding the non-ancestral Glycine residue

A predicted glycine at residue 674 of *ELF3-B1*, associated with late heading, is globally rare in wheat. In the 1000Exome data (33) 4.87% of lines have the predicted glycine residue and in the wheat HapMap panel (34) only Rialto has the predicted glycine residue out of the 62 globally diverse lines analysed (S2 Table). Similarly, of the 14 hexaploid varieties currently available from the 10+ Wheat Genome project only three (Cadenza, Paragon, ArinaLrFor) possess the non-ancestral glycine residue (S2 Table). However, analysis of multiple datasets (see methods) shows the non-ancestral glycine674 is more common in wheat varieties with a UK pedigree (9/13 varieties) (S3

Table). Alignment of *TaELF3* orthologues shows that the predicted serine residue is also conserved across monocots.

When looking for other potentially causal sequence variation we found that within the *ELF3-B1* promoter regions of Claire, Robigus, Paragon and Cadenza there are two sites polymorphic for cytosine repeat number ($(C)_n$) located 1967 bp and 1151 bp upstream of the transcriptional start site (TSS) (Fig 2B). As Robigus and Claire have an early flowering phenotype at the *Eps-B1* locus and Cadenza a late flowering phenotype (30) it is unlikely that the promoter $(C)_n$ polymorphisms cause the changes in heading dates because there is only a difference in two cytosines at the 1967 bp $(C)_n$ site between Cadenza and Robigus/Claire (Fig 2B). Furthermore *ELF3-B1* on Julius, Lancer, Mace, Norin61 and Sy Mattis seem to be inverted compared to ArinaLrFor, CDC Landmark, CDC Stanley, Chinese Spring and Jagger. However as none of these lines share the same haplotype with ArinaLrFor and Paragon (which both carry the Ser674Gly SNP) at *ELF3-B1* it is unlikely that an inversion is the cause behind the *Eps-B1* QTL. Thus, we conclude that the Ser674Gly SNP in *ELF3-B1* is the best candidate to underlie *Eps-B1*.

Subtelomeric introgression and inversion might underlie the *Eps-D1* heading date QTL

For the QTL located at *Eps-D1*, the Xi-19 haplotype caused an acceleration of heading ($p = 0.013$) (S1 Table). A subtelomeric deletion in Cadenza was previously described as the causal polymorphism underlying the *Eps-D1* locus (13,14) however by analysing data from recently published wheat assemblies (35) we discovered that this region is not deleted and suggest that the causal polymorphism may instead result

from a subtelomeric inversion derived from introgressed material. A BLAST search of the Chinese Spring *TaELF3-D1* genomic sequence against the 10+ Wheat Genome Project varieties identified high confidence matches in all varieties including Jagger and Cadenza. However, the sequence identity of the Jagger and Cadenza coding sequence for TraesJAG1D01G492900.1 and TraesCAD_scaffold_026352_01G000400.1 compared to the Chinese Spring gene is much lower (96.72%) than for the remaining 1D coding sequences (>99.9%). The Jagger and Cadenza 1D coding sequences have a greater similarity to the Chinese Spring *TaELF3-A1* (97.50%) and Chinese Spring *TaELF3-B1* (97.88%) homoeologues than to Chinese Spring *TaELF3-D1*.

Visualisation of the 1D chromosome for the 10+ Wheat Genome Project varieties using the Crop Haplotypes viewer (36) showed a shared haplotype block at the distal end of chromosome 1D between Cadenza (Haplotype viewer coordinates: 482.8 Mbp – 495.4 Mbp) and Jagger (480.0 Mbp to 493.5 Mbp) where *TaELF3-D1* is found.

The Cadenza v1.1 reference sequence has yet to be assembled into chromosomes, but since the Crop Haplotypes viewer (36) data indicated IBS with Jagger, we compared the distal end structure of the Jagger 1D chromosome with Chinese Spring. The end of the Jagger chromosome contains an inversion of approximately 2.6 Mbp relative to Chinese Spring which includes *TaELF3-D1* (Fig 4A). Alignment of the Jagger/Cadenza *TaELF3-D1* genomic sequence with Chinese Spring *TaELF3-D1* showed some sequence differences including a deletion within intron 2 (Fig 4B, S4 Table). Of the eight MAGIC parents only Xi-19, whose pedigree is CADENZA/RIALTO//CADENZA, has the Cadenza/Jagger *TaELF3-D1* allele (Fig 4C

and D). A PCR assay using the subgenome specific primers detailed in Fig 4B that amplify the region of *TaELF3-D1* containing intron 2 found the Cadenza/Jagger intron 2 deletion is also present in *Aegilops speltoides* and *Triticum timopheevii* (S2 Fig).

Given the low sequence conservation of the *TaELF3-D1* gene in Cadenza and Jagger and the presence of the intronic deletion in *Aegilops speltoides* and *Triticum timopheevii*, we investigated if the Cadenza/Jagger haploblock was an introgression. Reconstructing the phylogeny of the 1D Jagger/ Cadenza region using the 820k SNP dataset from CerealsDB showed that several Tonic descendants (Spark, Xi-19 Cadenza (Fig 4), KWS-Podium, Cordiale, Gallant, Duxford) as well as five others (Moisson, Bacanora, Tuerkis, Badger, Pavon) clustered separately from the remaining *T. aestivum* cultivars (S1 Fig). These lines also cluster with six Watkins lines from India (Watkins34), Yugoslavia (Watkins352), China (Watkins141), UK (Watkins103), Cyprus (Watkins292) and Turkey (Watkins299). *T. timophevii* clusters closely with the above lines. Gene alignment of *ELF-D1* orthologues and alignment of 300kb surrounding *ELF3-D1* also supports an origin outside the D genome for the Jagger/ Cadenza *ELF3-D1* gene (S3 Fig, S5 Table).

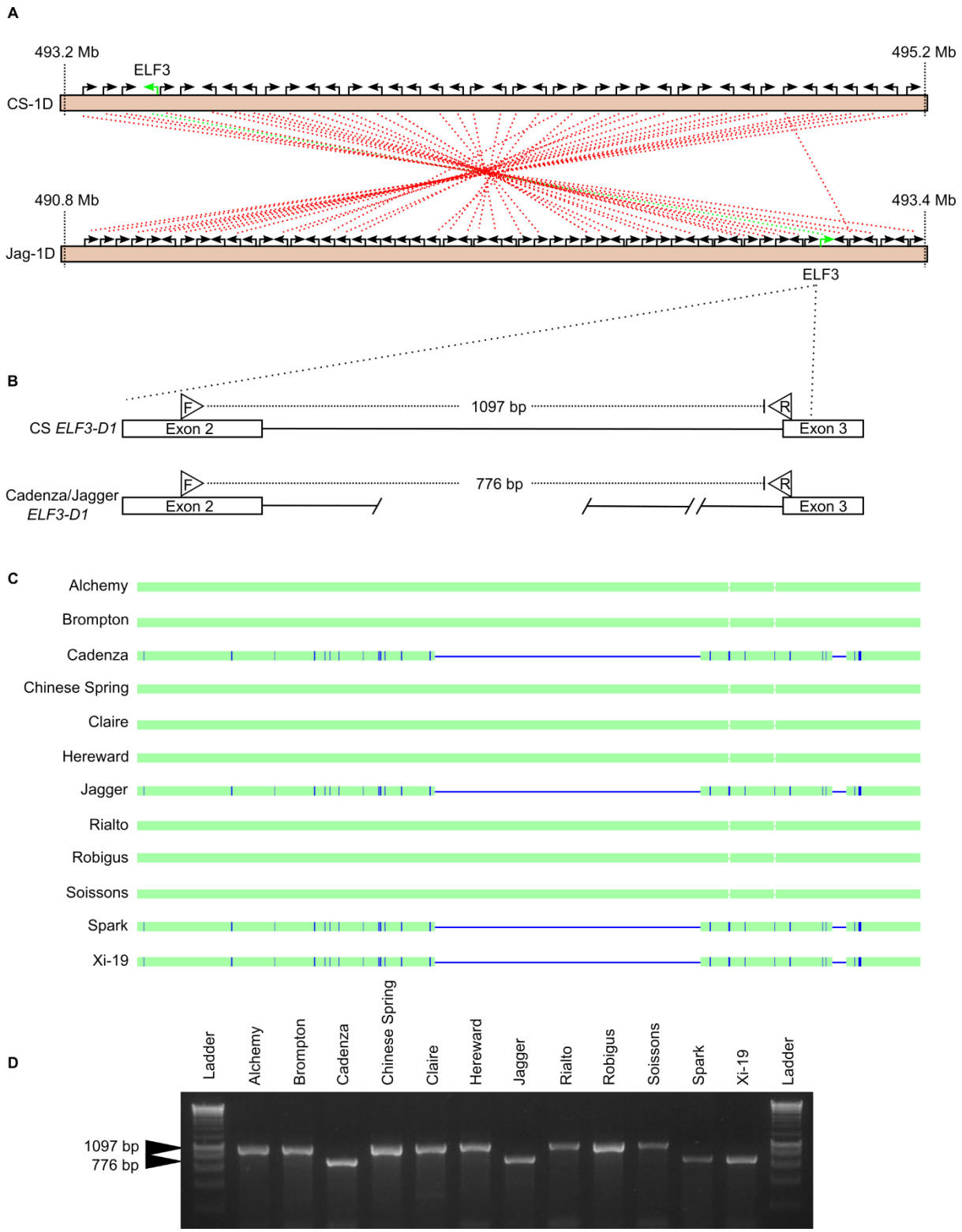

Fig 4. A subtelomeric chromosomal introgression and inversion containing *ELF3-D1* is likely to be the causal polymorphism underlying the *Eps-D1* QTL.

(A) Syntenic relationships between the distal end of Chinese Spring (CS) 1D chromosome (IWGSCv1.1) and Jagger (Jag) 1D (PGSBv2.0), *TaELF3-D1* highlighted in green, each black arrow corresponds to a gene in the forward (pointing right) or reverse (pointing left) strand. (B) the Cadenza/Jagger *ELF3-D1* contains a deletion within intron 2 which is not present in CS, F and R refer to relative primer binding sites for PCR amplification shown in (C). (D) Agarose gel separation of PCR products from (C). A PCR product at 776bp is indicative of the presence of a subtelomeric chromosomal introgression and inversion.

Allelic variation in *TaELF3* had no detectable effect on circadian rhythms in the MAGIC founder varieties

We investigated if the variation at *TaELF3-B1* and *TaELF3-D1* in the MAGIC parents, or other *loci,* might affect circadian rhythms in a manner that might explain the effects on heading date. We quantified circadian rhythms in the MAGIC founder varieties by measuring the period and amplitude of rhythms of delayed chlorophyll fluorescence (DF) in otherwise constant light (37). We detected robust circadian rhythms of DF in all the MAGIC parent lines (RAE < 0.5) (Fig 5A). Hereward had the shortest circadian period (25.0 h) (Fig 5C) and Xi-19 the longest period (26.2 h) but the difference between these periods and the global mean was not significant ($p = 0.132$) (Fig 5C). Because there was no significant difference in circadian period, we conclude that the allelic diversity in homeologues of *TaELF3* affected heading date without causing detectable changes in circadian rhythms.

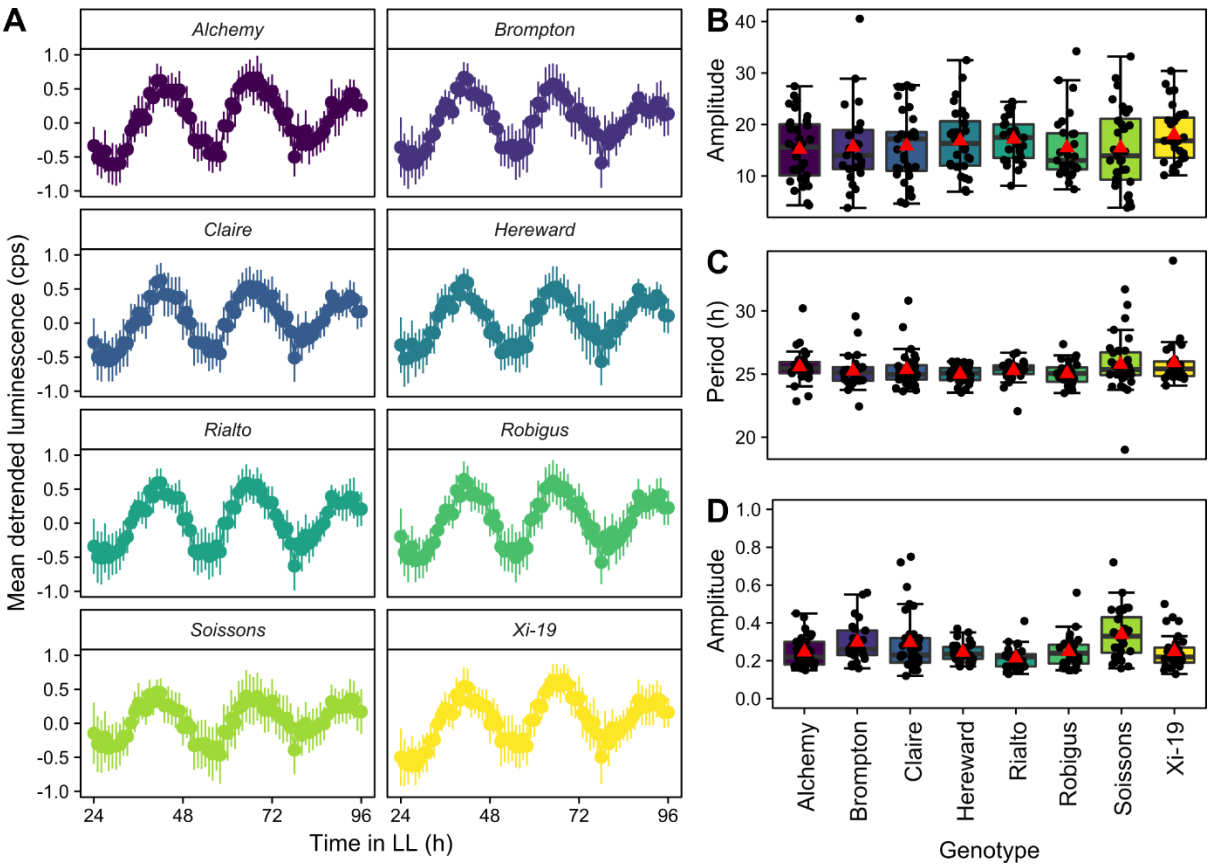

Fig 5. Circadian rhythms of delayed chlorophyll fluorescence in the MAGIC parents. (A) Mean DF luminescence in counts per second (cps) normalised to -1 to 1 using Biodare2 with error bars representing standard deviation (n = 27 - 33). Circadian amplitude (B), period (C) and RAE (D) calculated using FFT-NLLS (Biodare2). Upper and lower hinges represent the first and third quartiles (25th and 75th percentiles), the middle hinge represents the median value, red triangle represents mean value and black dots represent individual replicates

Loss of function mutation of *TtELF3* disrupts wheat circadian clocks

Because we found that variation in the MAGIC population at *TaELF3* was not correlated with a detectable effect on circadian rhythms, we examined whether *ELF3* is a circadian oscillator component in wheat. We obtained a tetraploid TILLIING mutant line carrying point mutations encoding stop codons in both *TtELF3-A1* and *TtELF3-B1* (30) herein designated *Ttelf3*-null (S4 Fig). We quantified circadian rhythms of

“prompt” chlorophyll *a* fluorescence (PF) (38) and leaf temperature under continuous light in both the *Ttelf3*-null and the respective *TtELF3*-WT obtained from the initial mutant TILLING line (30). We detected circadian rhythms in *TtELF3*-WT but *Ttelf3*-null was arrhythmic for all measures of PF (Fig 6C and S7 Fig) including $F_{m'}$ (*TtELF3*-WT RAE 0.36 ± 0.03; *Ttelf3*-null RAE 0.82 ± 0.08) (Fig 6C), leaf temperature (*TtELF3*-WT RAE 0.20 ± 0.04; *Ttelf3*-null RAE 0.56 ± 0.10) (Fig 6D-F) and DF (S5 Fig). The mean peak phase of relative leaf temperature for *TtELF3*-WT (Fig 6D) was 20.0 ± 0.2 h after subjective dawn, indicating, as expected, that stomata were most closed during the middle of the subjective night.

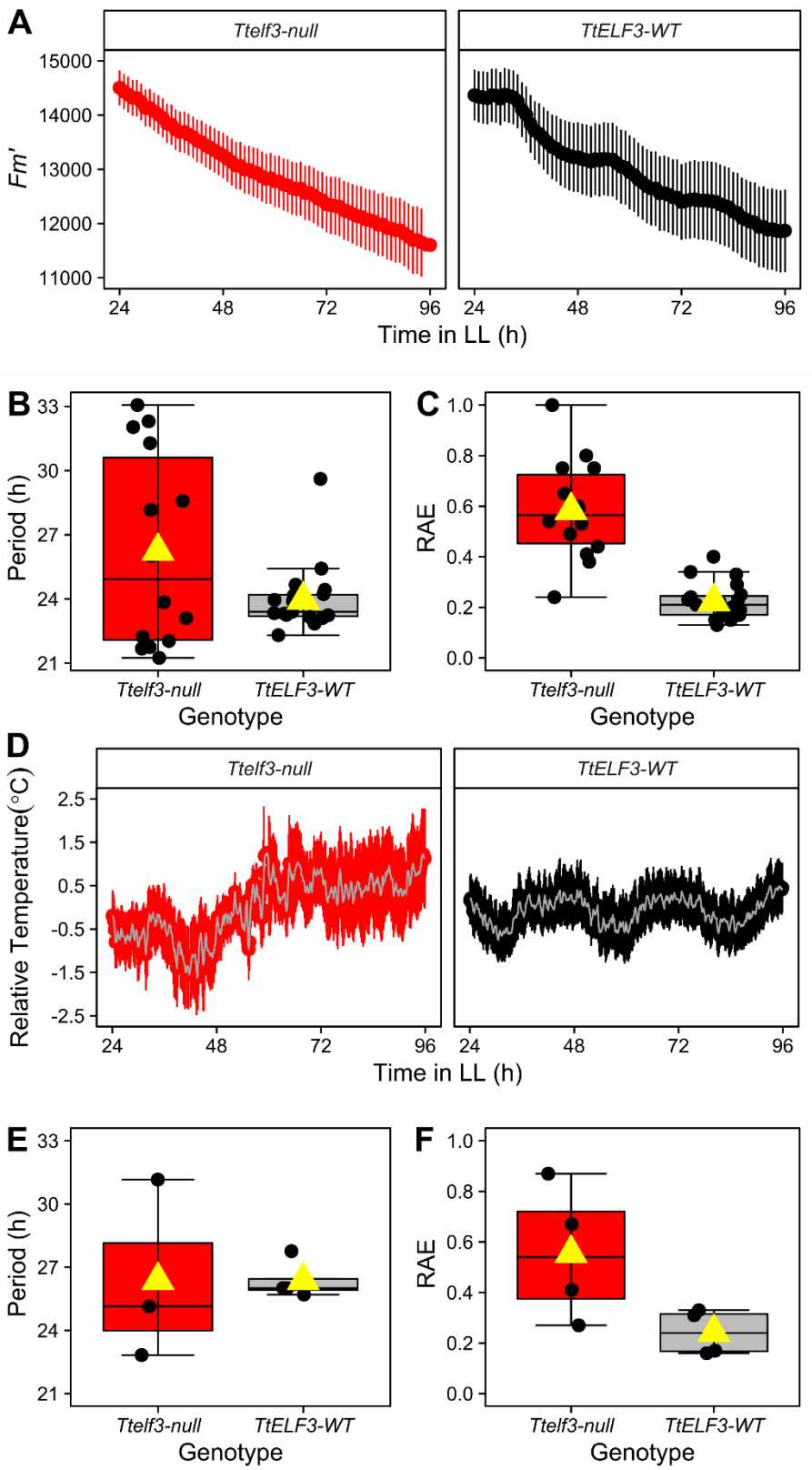

Fig 6. *Ttelf3*-null is arrhythmic in continuous light.

(A) Mean *Fm'* of *Ttelf3*-null (red) and *TtELF3-WT* (black) in LL (n = 24) (B) Mean period length (hours) and (C) RAE values for plot (A). Upper and lower hinges represent the first and third quartiles (25th and

75th percentiles), the middle hinge represents the median value, yellow triangle represents mean value and black dots represent individual replicates. (D) Mean leaf surface temperature relative to background and normalised to the mean in LL and constant environmental temperature (20°C) for *Ttelf3-null* (red) *TtELF3-WT* (black) and *Ttelf3-null* (red) (n = 4) (E) Mean period length and (F) RAE for plot (D). For clarity every 20th point plotted in (D). Error bars represent SEM.

Loss of functional *TtELF3* perturbs circadian oscillator gene expression in light dark cycles and constant light

To further investigate the function of *ELF3* in the wheat circadian system we measured the abundance of transcripts of orthologues of the Arabidopsis circadian oscillator components *LHY, TOC1, Ppd-1* (*PRR37*)*, PRR73, GI, ELF3* and *LUX* in light dark (LD) and continuous light (LL) cycles. In LD cycles all transcripts had rhythmic expression (Fig 7A-G). Consistent with previous findings in Arabidopsis, *TtLHY* had peak expression at dawn (Fig 7A), the *PRR* orthologues peaked during the photoperiod (Fig 7B-C) with *TtTOC1* (Fig 7D), *TtGI* (Fig 7E) and *TtLUX* (Fig 7F) peaking around dusk. However, the peak in *TtELF3* abundance was at the end of the night just prior to dawn (Fig 7G), approximately antiphase to the expression of *TtLUX* (Fig 7F). This differs markedly from Arabidopsis in which *ELF3* and *LUX* are co-expressed near dusk (7,39,40). For all transcripts, except *Ppd-1* (Fig 7B), we detected oscillations in transcript abundance in constant light, with the phasing in LL consistent with that in LD. These oscillations of circadian transcript abundance were abolished or of very low amplitude in *Ttelf3*-null (Fig 7A-G). There was a phase advance in peak transcript abundance of approximately 3 h in LD in *Ttelf3*-null compared to *TtELF3-WT* (Fig 7A-G) except for *TtELF3* transcript abundance where the peak phase was at dawn in both *TtELF3*-WT and *Ttelf3*-null (Fig 7G). The amplitude of transcript abundance under diel conditions was also less in the *Ttelf3*-null line compared to

ELF3-WT (Fig 7). Together, these data demonstrate that functional *TtELF3* is required for the maintenance of robust oscillations of circadian oscillator gene expression in LL and for normal circadian timing in LD.

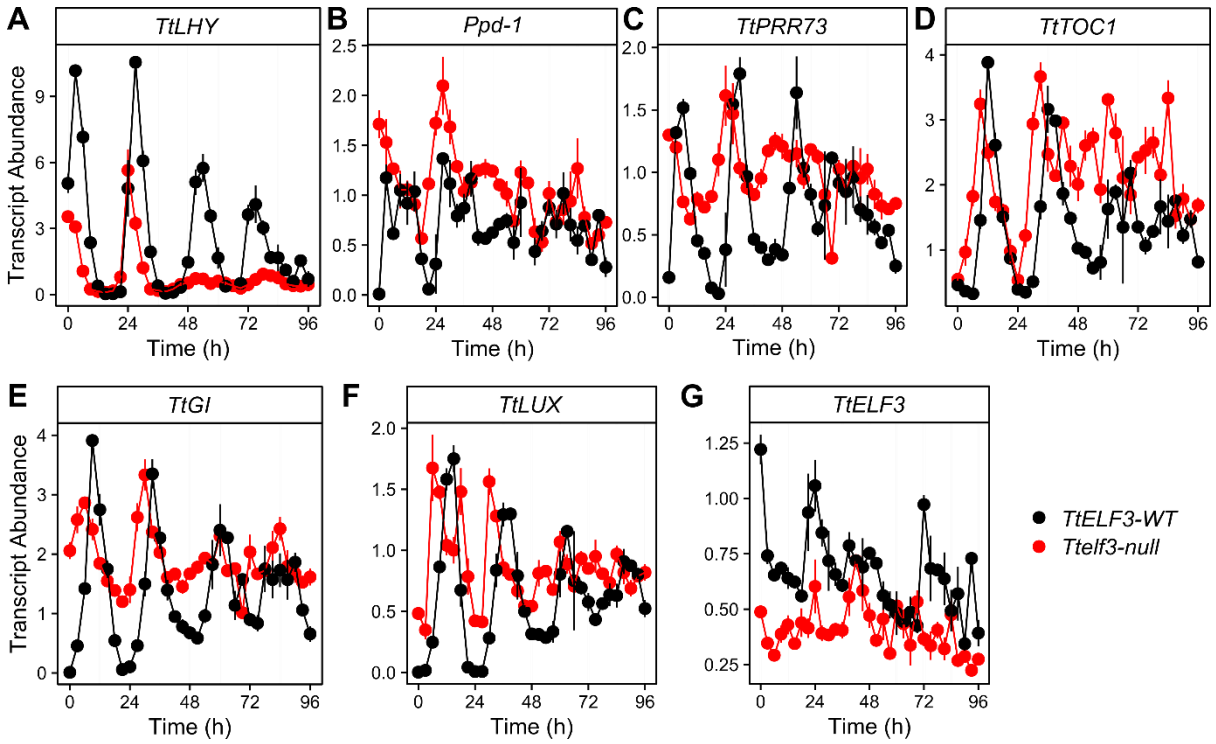

Fig 7. Abundance of wheat circadian clock transcripts in the *TtELF3-WT* and *ttelf3* lines in LD and LL.

(A-G) Mean abundance of circadian oscillator transcripts (n= 3 - 5) in *TtELF3*-WT (black) and *Ttelf3*-null (red) in a 24 h LD cycle in long day conditions (16 h light at 250 µmol m^{-2} s^{-1}, 20°C: 8 h dark 16°C, represented by vertical grey bar) followed by constant light and temperature (20°C) from time 24 to 96 h. Transcript abundance (ΔΔCq) is relative to *TtRP15* and *TtRPT5A* (A) *TtLHY,* (B) *Ppd-1,* (C) *TtPRR73,* (D) *TtTOC1,* (E) *TtGI,* (F) *TtLUX* and (G) *TtELF3* .

LUX loss of function disrupts the wheat circadian clock

The antiphase expression of wheat *ELF3* and *LUX* raises the possibility that the EC might not be formed, or functions differently to that in Arabidopsis. Previous studies in

diploid wheat have identified *TmLUX* as a circadian oscillator gene (17) so we investigated whether *LUX* also contributes to circadian rhythms in hexaploid wheat, and whether functionality of one homoeologue is sufficient to maintain robust oscillations. We obtained three hexaploid Japanese cultivars, Chogokuwase, Minaminokomugi and Geurumil that have variation at *TaLUX* associated with flowering time (41). Chogokuwase is an extra early flowering variety and is the offspring of Geurumil and Minaminokomugi. Chogokuwase carries predicted non-functional mutations in all three sub-genome copies of *TaLUX* (S8 Fig). Chogokuwase also carries a *TaVRN-D1* spring allele and a photoperiod insensitive *Ppd-D1a* allele. Geurumil has the same predicted non-functional alleles of *TaLUX* and *Ppd-D1a* but has a winter growth habit due to lacking the *VRN-D1* spring allele. Minaminokomugi carries the non-functional *Talux-a1* allele but wild-type alleles of *TaLUX-B1* and *TaLUX-D1* in addition to carrying the *TaVRN-D1* and *Ppd-D1a* alleles (42).

Minaminokomugi maintained robust oscillations of chlorophyll fluorescence (RAE 0.16 ± 0.01) and leaf temperature (RAE 0.26 ± 0.02) (Fig 8A-C). In contrast Chogokuwase, which lacks functional copies of *TaLUX,* was arrhythmic for PF (RAE 0.56 ± 0.06) and Geurumil, which is also lacking functional *TaLUX*, had reduced robustness of PF oscillations (RAE 0.33 ± 0.05) compared to Minaminokomugi (Fig 8A-C). Similarly, there was a decreased robustness of oscillations in leaf surface temperature for Chogokuwase and Geurumil (RAE 0.48 ± 0.09 and RAE 0.46 ± 0.11) which appeared to dampen to arrhythmia after the first two true LL cycles (Fig 8D-F). We conclude that functional *TaLUX* is required for robust circadian rhythms in hexaploid wheat.

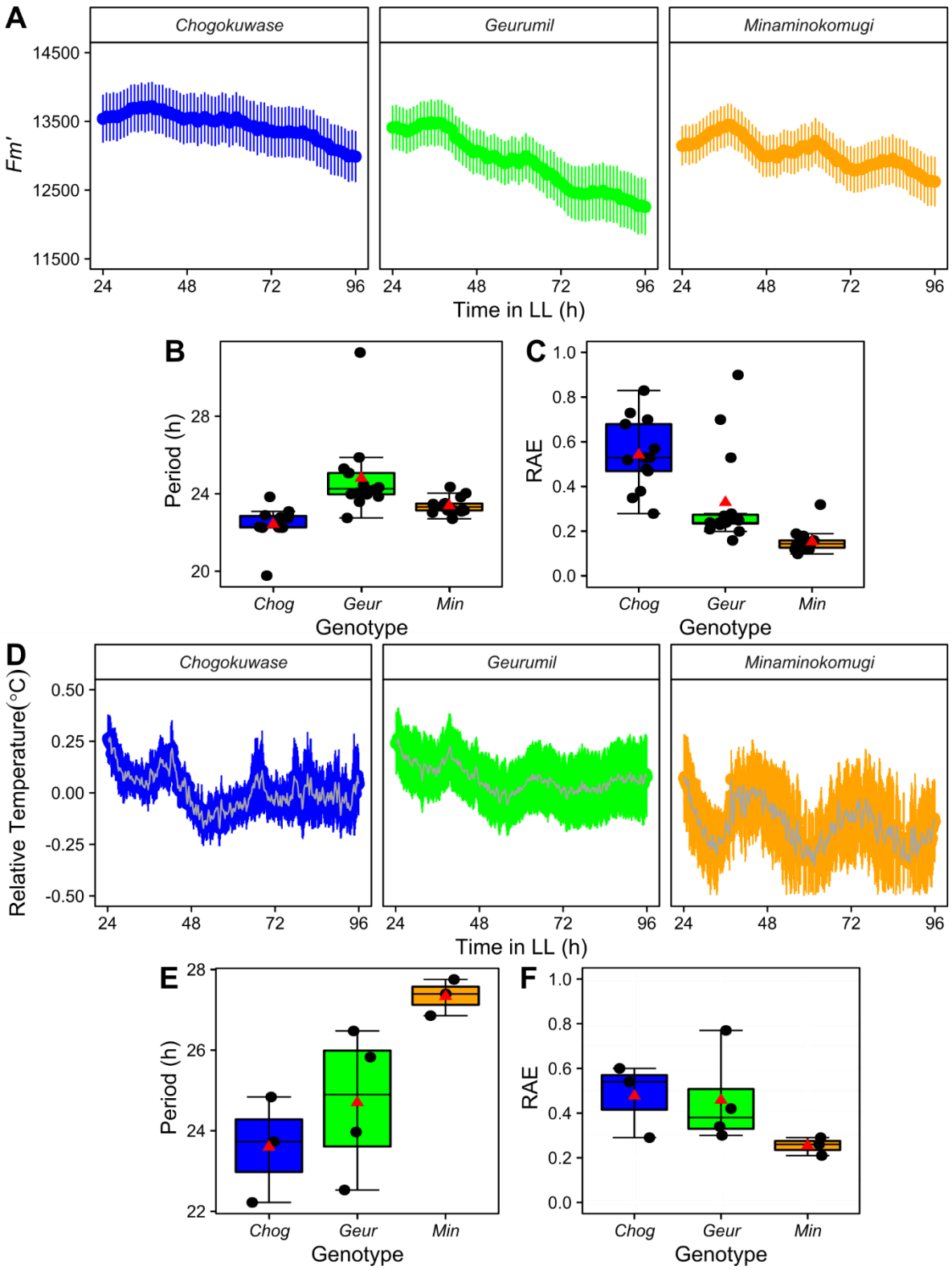

Fig 8. Functional *LUX* is required for maintenance of robust circadian oscillations under LL conditions in hexaploid wheat.

(A) Mean $F_{m'}$ for Chogokuwase (blue), Geurumil (green) and Minaminokomugi (orange) in LL (n = 16) (B) Mean period and (C) RAE for (A) calculated using FFT-NLLS (Biodare2). Upper and lower hinges represent the first and third quartiles (25th and 75th percentiles), the middle hinge represents the median value, red triangle represents mean value and black dots represent individual replicates. (D) Mean Chogokuwase, Geurumil and Minaminokomugi leaf temperature relative to background in LL (n = 4). (E) mean period and (F) RAE for plot (D). Error bars are SEM, for (D) every 20th point plotted for clarity.

Discussion

Different contributions of wheat sub-genomes to heading date and circadian rhythms

The eight MAGIC parent varieties provided the opportunity to measure the likely contribution of the *ELF3* homoeologues to heading date and circadian rhythms. Of the MAGIC parents Brompton, Hereward, Rialto and Xi-19 have a G|G substitution variant of *TaELF3-B1* and in addition Xi-19 has an inverted copy of *TaELF3-D1* likely arising from a past introgression event. These variations in *TaELF3* alleles had no discernible impact on circadian rhythms (Fig 5) but had measurable effects on heading date in the field (Fig 3).

Consistent with previous studies we conclude that *ELF3* underlies *Eps-B1* and is a candidate for *Eps-D1 loci* (13). We have extended the findings concerning the *Eps-D1* locus by demonstrating that a copy of *ELF3-D1* is present in Cadenza and Xi-19 varieties but lies within an introgression region that contains an inversion relative to the Chinese Spring D genome (Fig 4). Based on analysis of the 820k SNP data we find that a number of descendants of the cultivar Tonic carry the putative introgression, as do several other unrelated cultivars and six Watkins lines from India, China, UK,

Cyprus, Turkey and Yugoslavia. As a result, we hypothesise that this region predates modern breeding efforts. The same genomic region has been identified as being under selection in a collection of bread wheat accessions dating from 1790 to 1930, though in that study it was presumed to be a deletion rather than introgression (43). While the origin of the introgression is uncertain, the presence of Jagger/Cadenza *TaELF3-D1* intronic deletion in *Ae. speltoides* and *T. timopheevii* (S2 Fig) and the clustering outside of *Aegilops tauschii* lines (S1 and S3 Figs) supports an origin outside of the D genome, closer related to the G or S genome. The increase in quantity and quality of genomic resources for diverse accessions and wheat relative species will help in determining the origin of this introgression.

Our data also identify *ELF3-B1* as a candidate gene underlying the *Eps-B1* locus. We found that a predicted glycine674 in *TaELF3-B1,* which segregates with *Eps-B1,* caused a delay in flowering compared to the ancestral serine674 variant (Fig 3), in agreement with previous observations in Avalon (13). It was previously concluded that G|G is the ancestral variant (13) but our evidence suggests that it is more likely that A|A is ancestral because the G|G allele is globally rare, present in 4.87% of lines included in the 1000 Exome dataset, in one of the 62 wheat HapMap panel lines (S2 Table) and in three of the 14 10+ Wheat Genome project lines (S2 Table) and the ancestral serine residue is highly conserved, present in all sequenced grasses. However, within UK wheat germplasm (as defined by locality on wheat GRIS) the G|G allele is more common and is found in nine of the 13 UK lines we have investigated (S3 Table).

We found that the allelic variation at *TaELF3* which affected wheat heading date had no detectable effect on circadian rhythms but loss of functional *TtELF3* caused arrhythmia of PF (Fig 6A-C & S7 Fig), leaf temperature (Fig 6D-F) and gene expression in LL (Fig 7), and this loss of function caused advanced circadian phase in LD. This demonstrates that one role of *ELF3* is to contribute to the correct alignment of internal phase to external phase, which is a primary function of circadian oscillators. The earlier phasing of gene expression in LD cycles is similar to barley containing the *eam8.*w allele where the peak phase of *HvCCA1, HvTOC1* and *HvGI* expression was also earlier (11). Similarly, the loss of rhythmic oscillations in gene expression upon transition to LL was found in barley (11). We found that functional *TtELF3* is required for high amplitude *TtLHY* rhythms, and that *TtELF3* loss of function mutants have increased trough transcript abundance of *TtGI* (Fig 7E). The similarity of these observations to those in barley and rice lines carrying *ELF3* mutations (44,45) suggests that *ELF3* genes might have similar functions across grasses.

Taken together these results demonstrate separable effects of allelic variation at *TaELF3* on flowering time and circadian function with differential contributions of *TaELF3* homoeologues to heading date. Possibly, regulation of heading date is *ELF3*-dosage dependent whereas circadian period is buffered against dosage effects which would explain why complete loss of function of *ELF3* is required for a quantifiable change in circadian phenotype. It might be that that *ELF3* can affect heading in a circadian-independent manner through the regulation of gibberellin production, as occurs in barley (45).

An altered role for the evening complex in wheat

Binding of the Arabidopsis EC to target promoters requires LUX as both ELF3 and ELF4 lack DNA binding domains, and it is thought this might explain the similar timing of the transcript accumulation (7). However, in wheat the maximal abundance of *ELF3* and *LUX* transcripts is separated by 12 hours (Fig 7F and G). This difference in the peak time of *ELF3* and *LUX* transcript abundance also occurs in *T. monococcum* (30) and rice (44) and therefore may be a general feature of cereal circadian oscillators. Wheat also lacks a clear orthologue of *AtELF4* and instead contains *ELF4-like* genes (46). *ELF4-like* genes might have a conserved role because expression of a barley *ELF4-like* gene restored circadian rhythms to an Arabidopsis *elf4-2* mutant (47). There is further evidence for conservation of EC function in monocots because Brachypodium ELF3 binds Arabidopsis ELF4 and LUX, and can complement Arabidopsis *elf3-2* mutants (48). The temporal separation of wheat *ELF3* and *LUX* transcript abundance does not preclude the formation of an EC complex, but could suggest one is not formed, or occurs at a different time in the diel cycle to Arabidopsis. Whether through an EC or not, our data demonstrate that functional *ELF3* and *LUX* are required for robust circadian rhythms in wheat (Figs 6- 8).

The difference in timing of *TaELF3* and *TaLUX* expression compared to their Arabidopsis orthologues might arise as a consequence of promoter sequence differences. Within 5000 bp upstream of the three *TaELF3* homoeologues transcription start sites the most common motifs are linked to morning phased expression (38 morning, 20 evening and 8 midnight) (S6 Table). The general composition of the *TaELF3* promoters is similar to *TaLHY* (17 morning, 10 evening and 3 midnight) (S7 Table) but different to the evening expressed *TaLUX* promoters where the most

abundant motifs are associated with evening phased expression (34) compared to morning (21) and midnight (12) (S8 Table). In particular, *TaELF3* promoters contain Morning Element 1 (ME1) and Morning Element 2 (ME2) motifs, associated with morning phased expression (49), which are also found in the promoter region of the dawn expressed *TaLHY* homoeologues (S7 Table), but are absent in the *AtELF3* promoter (S6 Table). The *TaELF3* promoters also contain further morning-related motifs such as the multiple Hormone up at dawn 1 (HUD1) and Hormone up at dawn 2 (HUD2) elements (50) which are less frequent in the *AtELF3* promoter (S6 Table).

Wheat *ELF3* might be a promising breeding target

The separation of effects of homoeologous copies of *ELF3* on heading and circadian rhythms might make it a suitable target for breeding new lines with heading date better adapted to the local environment in the practice of chronoculture (2). In other species such as pea, lentil and barley, allelic variation in *ELF3* has permitted the cultivation of these crops at different latitudes (51–53). Whilst complete loss of functional *ELF3* in wheat significantly advances flowering time, severely disrupts circadian rhythms and decreases the spikelet number (30), we have demonstrated that altering the function of particular homoeologues of *ELF3* can affect heading but if some functional homoeologous copies of *ELF3* are present this can be achieved without a measurable disruption to the circadian oscillator and the associated potential yield penalties (54). It might be possible that by combining different alleles of *ELF3* with alleles of other circadian clock genes, flowering time can be precisely tuned to suit the growing environment. By using selected lines from the Cadenza TILLING population (55) it might be possible to better understand the effects of the Ser674Gly SNP in *TaELF3-B1* and the 1D introgression, as Cadenza contains both, in conjunction with other

mutations. In addition to the *ELF3* alleles described in this work, we have also identified further *ELF3* alleles including the absence of *ELF3-A1* in Julius (S9 Table) highlighting a range of *ELF3* alleles within modern wheat cultivars which could be incorporated into breeding programmes. The variation at *ELF3* might have occurred because of the positioning of *ELF3* within the subtelomeric region (56) which has enhanced levels of recombination which can lead to increased number of sequence and structural variants. This has been observed for other regions, recent studies have reported that a deletion at the distal end of chromosome 4AL is associated with altered heat tolerance (57) and a deletion at the distal end of 5AL encompasses the *Rht12* locus which is associated with dwarfing (58). Secondly, variation at *ELF3* may have been selected by past breeding efforts, leading to a change in allele frequencies, due to advantageous adaptation of flowering time to local climates similar to that seen for selection of *Ppd-1* alleles based on latitudinal cline (59) and altitude (60). A more systematic understanding of circadian clock gene alleles and their combinations will allow for a more targeted approach in optimising flowering time without impacting the functioning of the circadian clock.

Materials and methods

Plant material

The eight MAGIC parents; Alchemy, Brompton, Claire, Hereward, Rialto, Robigus, Soissons and Xi-19 were obtained from NIAB (National Institute of Agricultural Botany, UK). The *Ttelf3*-null and *TtELF3*-WT lines were donated by Jorge Dubcovksy (30) where the *Ttelf3*-null line is the progeny of bulked *elf3-null/Ppd-A1b* and the *TtELF3*-WT line is progeny of bulked *ELF3WT/Ppd-A1b* (Table 3). The Chogokuwase, Minaminokomugi and Geurumil lines were donated by Hidetaka Nishida (41).

Table 3: Wheat lines used in this study. GRU refers to the germplasm resource unit at the John Innes Centre, Norwich.

Species	Cultivar	Genotype	Reference
Ae. speltoides			GRU 2140023
T. aestivum	Alchemy		(3)
T. aestivum	Brompton		(3)
T. aestivum	Claire		(3)
T. aestivum	Hereward		(3)
T. aestivum	Rialto		(3)
T. aestivum	Robigus		(3)
T. aestivum	Soissons		(3)
T. aestivum	Xi-19		(3)
T. aestivum	Cadenza		GRU WBCDB0013-PG1
T. aestivum	Jagger		GRU PANG0006
T. aestivum	Spark		GRU WBCDB0052
T. aestivum	Chinese Spring		
T. aestivum	Chogokuwase		(42)
T. aestivum	Minaminokomugi		(42)
T. aestivum	Geurumil		(42)
T. monococcum			GRU T1040057
T. sphaerococcum			GRU 1210007
T. timopheevii			GRU 116002
T. turgidum	Kronos	*Ttelf3*-null line	(30)
T. turgidum	Kronos	*TtELF3*-WT	(29)

Plant growth conditions

Seeds were surface sterilized by washing once in 70% (v/v) ethanol for one minute (Fischer Scientific, UK), once in autoclaved water for one minute, followed by 15 minutes in 10% (v/v) sodium hypochloride solution (Fischer Scientific, UK) and then washed a further three times in autoclaved deionized water. Seeds were sown directly onto 96 well modular trays (P G Horticulture Ltd, UK), containing a 1:1 mix of Levington M2 potting compost (Levington, UK) and vermiculite (fine, Willian Sinclair Horticulture, UK) and treated with the insecticide Intercept 70W (0.02 g L-1 soil, Bayer, Germany). Plants were grown in growth chambers (Conviron, Canada) under long days and constant temperature (16 h L: 8 h D; 200 µmol m^{-2} s^{-1}; 20 °C).

Field trials

In 2012/2013 a fully replicated yield trial of 784 F_5 MAGIC lines at the NIAB experimental farm in Cambridge, UK was scored by NIAB for the timing of Growth stage 39 (Flag leaf blade all visible), Growth stage 55 (Half of ear emerged above flag leaf ligule) and Growth stage 61 (start of flowering on main stem, approximately 1/3 of the way up the ear, with pollen visible) on the Zadok's scale (C., Chang and Konzak, 1974)(Mackay et al., 2014). Growth stage measurements were scored as days after sowing. In the 2013/2014 field season the same growth stage phenotypes were collected from a fully replicated yield trial of 784 F_6 MAGIC lines.

Analysis of field phenotypes

Asreml-R 3.0 (61) was used to minimize or remove spatial effects in phenotype data due to field variation.

Marker genotypes and their respective chromosomal groupings from (23) were used. The genetic map was reordered visually using the R package mpMapInteractive (62) to improve ordering and consider physical ordering information from IWGSCRefSeqv1. Recombination fractions were recalculated in mpMap (63) for each chromosome using mpestrf(). Recalculating recombination fractions on a per chromosome basis with the existing marker groupings significantly reduced computation resources required and enables the use of finer recombination bins (r <- c(0:5/600, 2:20/200, 11:50/100) compared to the default values. Genetic map lengths were recalculated using the Kosambi mapping function in computemap().

To reduce computational effort a skimmed genetic map with only unique mapping locations was used to calculate MAGIC line haplotypes and conduct QTL mapping in MPWGAIM only (26). A marker for each unique coordinate was chosen which had the lowest missing calls and preferably a clear BLAST hit to the IWGSCRefSeqv1 reference sequence, which was used to assign physical mapping coordinates. Out of 18089 mapped markers 4458 were chosen for downstream haplotype calculations.

Synteny analysis between Chinese Spring and Jagger 1D

A conserved haplotype block between Cadenza and Jagger at the distal end of chromosome 1D was identified using the Crop Haplotypes web browser (Crop Haplotypes (crop-haplotypes.com) (36). Physical locations of genes on the Chinese Spring 1D chromosome (IWGSCRefSeqv1.1) and Jagger 1D chromosome (PGSBv2.0) were mapped using the mapviewer v2.6.1 (https://10wheatgenomes.plantinformatics.io/mapview) and then confirmed manually using EnsemblPlants.

SNP mining and analysis

820k and 35k SNP array data was obtained from the CerealsDB website (64) and the 1000Exome data from the 1000 Exomes project website (http://wheatgenomics.plantpath.ksu.edu/1000EC/). Mapping of 35k and 820k SNPs to the IWGSCv1.1 Ref sequence were obtained from EnsemblPlantsv51. SNPs for the Cadenza/Jagger haplotype (chr1D: 482.3Mb – end of chromosome 1D) were extracted and heterozygous calls set as missing. Distance matrices and phylogenetic trees were constructed using the R package “ape” (65) 100 bootstrap permutations were run also using the R package “ape”.

To investigate the prevalence of the Ser674Gly SNP in a broad range of germplasm we analysed variation data from multiple sources including the 820k SNP genotyping array (66), the wheat HapMap panel (34), the 1000 wheat Exome project (He et al., 2019) and the 10+ Wheat Genome project (35). We found that the Ser674Gly SNP was also present in the HapMap panel as chr1B_685645813 and within the 1000 Exome data as scaffold48561_337271.

Phylogenetic tree construction

ELF3-D1 orthologous groups were retrieved from public repositories. Coding sequences were aligned using the MCoffee aligner on default settings (https://pubmed.ncbi.nlm.nih.gov/16556910/). Maximum Likelihood (ML) Phylogenetic trees were build using CLC Genomics Workbench 21.0.3. The best substitution model was determined using the Model testing function before running Molecular Phylogenetic analysis by Maximum Likelihood method with 100 permutations for Bootstrap values. The *ELF3* gene from *Brachypodium distachyon* was used as an outgroup.

Quantitative Real-Time PCR

The *TtELF3*-WT and *Ttelf3*-null lines were sown and grown in two antiphased LED growth chambers (Conviron) under long day conditions (16h L: 8h D; 250 µmol m^{-2} s^{-1}, 20°C day: 16°C night). Sampling commenced 16 days post-sowing, the first true leaf was sampled every 3 hours for 96 hours. After the first 24 hours of sampling the cabinet was switched to constant light and temperature (250 µmol m^{-2} s^{-1} , 20°C). Total RNA was extracted from leaf samples using the KingFisher Flex purification system

(Thermofisher scientific) in conjunction with the Maxwell® HT simplyRNA Kit (Promega). RNA concentration was determined using the Nanodrop ND-1000. DNA contamination was removed using the Arcticzyme HL-DNAse kit. RNA integrity was checked using the Fragment AnalyzerTM (AATI, USA) before cDNA was synthesised from extracted RNA using the High-Capacity cDNA reverse transcription kit (Applied Biosystems). Three technical replicates of gene specific products were amplified in 10 µl reactions using Power SYBR Green Master mix on a CFX384 Touch Real-Time PCR detection system. Gene expression levels were determined relative to the expression of two housekeeping genes that were selected using the GeNorm alogorithm (67) (Table 4).

Table 4: Primers used in this study

Gene	Sequence 5'-3'
TtCCA1	F: CCTGGAATTGGAGATGGAGA
	R: TGAGCATGGCTTCTGATTTG
TtELF3	F: TCTCCAGATGATGTTGTCGGT
	R: CTCGAACACTTGGACAGCAAA
TtGI	F: GGTAGGTGATAGACGGCACTT
	R: GTGCTACAGATGGGATGCTTG
TtLUX	F: ACAAGCGGTTCGTGGAGG
	R: CCTGCATCCGCTTGACGTA
TtPpd-1	F: CCTGTGGACTGTCGATCTCAA
	R: CAAGGGATGGCAGCGATAATG
TtPRR73	F: TCCCGAAGTTCCTCTCTTTCC
	R: AGCGGTAGTGGCAATGACA
TtTOC1	F: GGCATGGCACTTCATTCAGTT
	R: GCACATTCATACCAGCAGGAC
TtRP15	F: GCACACGTGCTTTGCAGATAAG
	R: GCCCTCAAGCTCAACCATAACT
TtRPT5A	F: GCTGGCTCGTTCAACTGATG
	R: GGACCAAGCGTTCTGATTACTC
TaELF3-D1	F: CAACGGCGCTTCTAATCTG
	R: AAACCCGCTGCTGACTGTATA

PCR of *ELF3-D1* in Cadenza and Xi-19

DNA extracted from the eight MAGIC parents, Cadenza and Chinese Spring using the DNeasy plant mini extraction kit (Qiagen, UK). The presence of *ELF3-D1* was confirmed by PCR using the *TaELF3-D1* primers listed in Table 4. PCR was performed using the DreamTaq Green PCR kit (Thermo Scientific, UK) on a ProFlex PCR system (Thermo Scientific, UK). PCR reaction conditions were as follows: 3 minutes at 95ºC; 40 cycles of 30 s at 95ºC, 30 s at 68ºC, 90 s at 72ºC; 15 minutes at 72ºC.

Delayed chlorophyll fluorescence and prompt chlorophyll *a* fluorescence imaging

Leaf samples were taken from the upper half of the first true leaf of 16 day old seedlings (non-vernalized) and were cut into 3 mm by 3 mm pieces and placed on solid 0.8% (w/v) bactoagar, 0.5 x MS Vitamin medium (M3900, Sigma-Aldrich, UK) supplemented with 0.5 µM benzyl-aminopurine (BAP), poured in a black 96 well imaging plates (Greiner, UK). Delayed fluorescence (37) was measured for 60s in an LB985 Nightshade (Berthold, UK) camera. Between measurements of DF light was supplied from blue (470 nm) red (660 nm) and LED arrays at 100 µmol m^{-2} s^{-1} during the experiment. Temperature was maintained at 20 ºC .

Chlorophyll *a* fluorescence and calculations of parameters were carried out using a CFimager (Technologica Ltd, Colchester, UK) and the image processing scripts provided by the manufacturer. Chlorophyll fluorescence images were captured using a Stingray F145B ASG camera (Allied Vision Technologies, UK) through an RG665 long pass filter to exclude blue light from the LEDs. When imaging under continuous

light, leaf fragments were exposed to 40 minutes of 100 µmol m^{-2} s^{-1} of blue light followed by a saturating pulse of 6172 µmol m^{-2} s^{-1} blue light for 800 ms then 20 minutes of darkness (with non-actinic measuring light on) followed by a second saturating pulse of 6172 µmol m^{-2} s^{-1} for 800 ms.

Circadian measures of amplitude, phase, period and relative amplitude error were calculated using the FFT-NLLS method in Biodare2 (www.biodare2.ed.ac.uk) (68). Where necessary data was normalised to between -1 and 1 using the normalisation feature of Biodare2.

Direct contact leaf temperature measurements

Leaf surface temperature relative to background temperature was measured using an in-house built device and provides an alternative measure of circadian rhythms caused by circadian regulated changes in the stomatal aperture (69). The temperature logger was validated by measuring circadian rhythms of “in-phase” and “anti-phase” wheat leaves where peak temperature, and therefore maximum closure, occurred during the subjective night (S6 Fig). Leaf temperature measurements were taken from fully expanded flag leaf of 4-week-old plants under continuous light and temperature (200 µmol m^{-2} s^{-1}, 20°C) that were previously grown under long days (16h L: 8h D; 200 µmol m^{-2} s^{-1}, 20°C day: 15°C night) in a growth cabinet (Conviron, UK).

Wheat was grown in 10 cm pots. Circadian measurements of leaf temperature were taken when the pants were four-weeks old. Type-K thermocouples were attached to the leaf such the end of the thermocouple was pressing onto the surface of the fully expanded flag leaf. This was kept in position by positioning a paperclip onto the leaf

and fixing the paperclip to a stake. The thermocouples were connected to an Arduino Mega using the Adafruit 1778, a 10 bit D-A converter and x20 amplifier giving a resolution of ± 0.1°C with a DS3231 RTC added to keep time, temperature was logged every 30s. Background temperature was measured using unattached thermocouples. Leaf temperatures were averaged using a 60-point moving average, background temperature was then subtracted from leaf temperature to give leaf temperature relative to background.

Bibliography

1. McClung C. The Plant Circadian Oscillator. Biology (Basel). 2019;8(1):14.
2. Steed G, Cano-Ramirez DL, Hannah MA, Webb AA. Chronoculture, harnessing the circadian clock to improve crop yield and sustainability. Science (80-). 2021;372(April).
3. Mackay IJ, Bansept-Basler P, Bentley AR, Cockram J, Gosman N, Greenland AJ, et al. An eight-parent multiparent advanced generation inter-cross population for winter-sown wheat: Creation, properties, and validation. G3 Genes, Genomes, Genet. 2014;4(9):1603–10.
4. Hawkesford MJ, Araus JL, Park R, Calderini D, Miralles D, Shen T, et al. Prospects of Doubling Global Wheat Yields. Food Energy Secur. 2013;2(1):34–48.
5. Gerland P, Raftery AE, Sevcikova H, Li N, Gu D, Spoorenberg T, et al. World population stabilization unlikely this century. Science (80-). 2014;346(6206):234–7.
6. Hsu PY, Harmer SL. Wheels within wheels: The plant circadian system.

Trends Plant Sci. 2014;19(4):240–9.

7. Nusinow DA, Helfer A, Hamilton EE, King JJ, Imaizumi T, Schultz TF, et al. The ELF4–ELF3–LUX complex links the circadian clock to diurnal control of hypocotyl growth. Nature. 2011;475(7356):398–402.

8. Herrero E, Kolmos E, Bujdoso N, Yuan Y, Wang M, Berns MC, et al. EARLY FLOWERING4 Recruitment of EARLY FLOWERING3 in the Nucleus Sustains the Arabidopsis Circadian Clock. Plant Cell Online. 2012;24(2):428–43.

9. Dixon LE, Knox K, Kozma-Bognar L, Southern MM, Pokhilko A, Millar AJ. Temporal repression of core circadian genes is mediated through EARLY FLOWERING 3 in Arabidopsis. Curr Biol. 2011;21(2):120–5.

10. Nagel DH, Kay SA. Complexity in the wiring and regulation of plant circadian networks. Curr Biol. 2012;22(16):648–57.

11. Faure S, Turner a. S, Gruszka D, Christodoulou V, Davis SJ, von Korff M, et al. Mutation at the circadian clock gene EARLY MATURITY 8 adapts domesticated barley (Hordeum vulgare) to short growing seasons. Proc Natl Acad Sci. 2012;109(21):8328–33.

12. Matsubara K, Ogiso-Tanaka E, Hori K, Ebana K, Ando T, Yano M. Natural variation in Hd17, a homolog of arabidopsis ELF3 that is involved in rice photoperiodic flowering. Plant Cell Physiol. 2012;53(4):709–16.

13. Zikhali M, Wingen LU, Griffiths S. Delimitation of the Earliness per se D1 (Eps-D1) flowering gene to a subtelomeric chromosomal deletion in bread wheat (Triticum aestivum). J Exp Bot. 2016;67(1):287–99.

14. Ochagavía H, Prieto P, Zikhali M, Griffiths S, Slafer GA. Earliness Per Se by Temperature Interaction on Wheat Development. Sci Rep. 2019;9(1):2584.

15. Kundu P, Sahu R. GIGANTEA confers susceptibility to plants during spot

blotch attack by regulating salicylic acid signalling pathway. Plant Physiol Biochem. 2021;167:349–57.

16. Sun H, Zhang W, Wu Y, Gao L, Cui F, Zhao C, et al. The Circadian Clock Gene, TaPRR1, Is Associated With Yield-Related Traits in Wheat (Triticum aestivum L.). Front Plant Sci. 2020;11:285.

17. Gawronski P, Ariyadasa R, Himmelbach A, Poursarebani N, Kilian B, Stein N, et al. A Distorted Circadian Clock Causes Early Flowering and Temperature-Dependent Variation in Spike Development in the Eps-3Am Mutant of Einkorn Wheat. Genetics. 2014;196(4):1253–61.

18. Campoli C, Pankin A, Drosse B, Casao CM, Davis SJ, Von Korff M. HvLUX1 is a candidate gene underlying the early maturity 10 locus in barley: Phylogeny, diversity, and interactions with the circadian clock and photoperiodic pathways. New Phytol. 2013;199(4):1045–59.

19. Beales J, Turner A, Griffiths S, Snape JW, Laurie DA. A Pseudo-Response Regulator is misexpressed in the photoperiod insensitive Ppd-D1a mutant of wheat (Triticum aestivum L.). Theor Appl Genet. 2007;115(5):721–33.

20. Shaw LM, Turner AS, Laurie DA. The impact of photoperiod insensitive Ppd-1a mutations on the photoperiod pathway across the three genomes of hexaploid wheat (Triticum aestivum). Plant J. 2012;71(1):71–84.

21. Bentley AR, Horsnell R, Werner CP, Turner AS, Rose GA, Bedard C, et al. Short, natural, and extended photoperiod response in BC2F4 lines of bread wheat with different Photoperiod-1 (Ppd-1) alleles. J Exp Bot. 2013;64(7):1783–93.

22. Turner AS, Faure S, Zhang Y, Laurie DA. The effect of day-neutral mutations in barley and wheat on the interaction between photoperiod and vernalization.

Theor Appl Genet. 2013;126(9):2267–77.

23. Gardner KA, Wittern LM, Mackay IJ. A highly recombined, high-density, eight-founder wheat MAGIC map reveals extensive segregation distortion and genomic locations of introgression segments. Plant Biotechnol J. 2016;14(6):1406–17.

24. Zadoks JC, Chang TT, Konzak CF. A decimal code for the growth stages of cereals. Weed Res. 1974;14(6):415–21.

25. Griffiths S, Simmonds J, Leverington M, Wang Y, Fish L, Sayers L, et al. Meta-QTL analysis of the genetic control of ear emergence in elite European winter wheat germplasm. Theor Appl Genet. 2009;119(3):383–95.

26. Verbyla AP, Cavanagh CR, Verbyla KL. Whole-Genome Analysis of Multienvironment or Multitrait QTL in MAGIC. G3 Genes|Genomes|Genetics. 2014;4(9):1569–84.

27. Camargo A V., Mott R, Gardner KA, Mackay IJ, Corke F, Doonan JH, et al. Determining Phenological Patterns Associated with the Onset of Senescence in a Wheat MAGIC Mapping Population. Front Plant Sci. 2016;7:1540.

28. Yao W, Li G, Yu Y, Ouyang Y. funRiceGenes dataset for comprehensive understanding and application of rice functional genes. Gigascience. 2018;1(7):1-9.

29. Faricelli ME, Valárik M, Dubcovsky J. Control of flowering time and spike development in cereals: The earliness per se Eps-1 region in wheat, rice, and Brachypodium. Funct Integr Genomics. 2010;10(2):293–306.

30. Alvarez MA, Tranquilli G, Lewis S, Kippes N, Dubcovsky J. Genetic and physical mapping of the earliness per se locus Eps-A m 1 in Triticum monococcum identifies EARLY FLOWERING 3 (ELF3) as a candidate gene.

Funct Integr Genomics. 2016;16(4):365–82.

31. Harper AL, Trick M, He Z, Clissold L, Fellgett A, Griffiths S, et al. Genome distribution of differential homoeologue contributions to leaf gene expression in bread wheat. Plant Biotechnol J. 2016;14(5):1207–14.

32. Clavijo BJ, Venturini L, Schudoma C, Accinelli GG, Kaithakottil G, Wright J, et al. An improved assembly and annotation of the allohexaploid wheat genome identifies complete families of agronomic genes and provides genomic evidence for chromosomal translocations. Genome Res. 2017;27(5):885–96.

33. He F, Pasam R, Shi F, Kant S, Keeble-Gagnère G, Kay P, et al. Exome sequencing highlights the role of wild-relative introgression in shaping the adaptive landscape of the wheat genome. Nat Genet. 2019;51(5):896–904.

34. Jordan KW, Wang S, Lun Y, Gardiner L-J, MacLachlan R, Hucl P, et al. A haplotype map of allohexaploid wheat reveals distinct patterns of selection on homoeologous genomes. Genome Biol. 2015;16(1):48.

35. Walkowiak S, Gao L, Monat C, Haberer G, Kassa MT, Brinton J, et al. Multiple wheat genomes reveal global variation in modern breeding. Nature. 2020;588(7837):277–83.

36. Brinton J, Ramirez-Gonzalez RH, Simmonds J, Wingen L, Orford S, Griffiths S, et al. A haplotype-led approach to increase the precision of wheat breeding. Commun Biol. 2020;3(1):1–11.

37. Gould PD, Diaz P, Hogben C, Kusakina J, Salem R, Hartwell J, et al. Delayed fluorescence as a universal tool for the measurement of circadian rhythms in higher plants. Plant J. 2009;58(5):893–901.

38. Dakhiya Y, Hussien D, Fridman E, Kiflawi M, Green R. Correlations between Circadian Rhythms and Growth in Challenging Environments. Plant Physiol.

2017;173(3):1724–34.

39. Huang H, Alvarez S, Bindbeutel R, Shen Z, Naldrett MJ, Evans BS, et al. Identification of evening complex associated proteins in arabidopsis by affinity purification and mass spectrometry. Mol Cell Proteomics. 2016 Jan 1;15(1):201–17.

40. Ezer D, Jung JH, Lan H, Biswas S, Gregoire L, Box MS, et al. The evening complex coordinates environmental and endogenous signals in Arabidopsis. Nat Plants. 2017;3(7).

41. Mizuno N, Nitta M, Sato K, Nasuda S. A wheat homologue of PHYTOCLOCK 1 is a candidate gene conferring the early heading phenotype to einkorn wheat. Genes Genet Syst. 2012;87(6):357–67.

42. Mizuno N, Kinoshita M, Kinoshita S, Nishida H, Fujita M, Kato K, et al. Loss-of-function mutations in three homoeologous PHYTOCLOCK 1 genes in common wheat are associated with the extra-early flowering phenotype. PLoS One. 2016;11(10):1–19.

43. Przewieslik-Allen AM, Wilkinson PA, Burridge AJ, Winfield MO, Dai X, Beaumont M, et al. The role of gene flow and chromosomal instability in shaping the bread wheat genome. Nat Plants. 2021;7(2):172–83.

44. Zhao J, Huang X, Ouyang X, Chen W, Du A, Zhu L. OsELF3-1 , an Ortholog of Arabidopsis EARLY FLOWERING 3 , Regulates Rice Circadian Rhythm and Photoperiodic Flowering. PLoS One. 2012;7(8):1–10.

45. Boden SA, Weiss D, Ross JJ, Davies NW, Trevaskis B, Chandler PM, et al. EARLY FLOWERING3 Regulates Flowering in Spring Barley by Mediating Gibberellin Production and FLOWERING LOCUS T Expression. Plant Cell. 2014;26(4):1557–69.

46. Calixto CPG, Waugh R, Brown JWS. Evolutionary Relationships Among Barley and Arabidopsis Core Circadian Clock and Clock-Associated Genes. J Mol Evol. 2015;80(2):108–19.

47. Kolmos E, Nowak M, Werner M, Fischer K, Schwarz G, Mathews S, et al. Integrating ELF4 into the circadian system through combined structural and functional studies. HFSP J. 2009 Oct;3(5):350–66.

48. Huang H, Gehan MA, Huss SE, Alvarez S, Lizarraga C, Gruebbling EL, et al. Cross-species complementation reveals conserved functions for EARLY FLOWERING 3 between monocots and dicots. Plant Direct. 2017;00:1–14.

49. Michael TP, Mockler TC, Breton G, McEntee C, Byer A, Trout JD, et al. Network Discovery Pipeline Elucidates Conserved Time-of-Day–Specific cis-Regulatory Modules. PLoS Genet. 2008;4(2):e14.

50. Michael TP, Mockler TC, Breton G, McEntee C, Byer A, Trout JD, et al. Network discovery pipeline elucidates conserved time-of-day-specific cis-regulatory modules. PLoS Genet. 2008 Feb;4(2):14.

51. Weller JL, Liew LC, Hecht VFG, Rajandran V, Laurie RE, Ridge S, et al. A conserved molecular basis for photoperiod adaptation in two temperate legumes. Proc Natl Acad Sci U S A. 2012;109(51):21158–63.

52. Zakhrabekova S, Gough SP, Braumann I, Muller AH, Lundqvist J, Ahmann K, et al. Induced mutations in circadian clock regulator Mat-a facilitated short-season adaptation and range extension in cultivated barley. Proc Natl Acad Sci. 2012;109(11):4326–31.

53. Lundqvist U. Scandinavian mutation research in barley - a historical review. Hereditas. 2014;151(6):123–31.

54. Dodd AN, Salathia N, Hall A, Kévei E, Tóth R, Nagy F, et al. Plant circadian

clocks increase photosynthesis, growth, survival, and competitive advantage. Science. 2005;309(5734):630–3.

55. Uauy C, Paraiso F, Colasuonno P, Tran RK, Tsai H, Berardi S, et al. A modified TILLING approach to detect induced mutations in tetraploid and hexaploid wheat. BMC Plant Biol. 2009;9(1):1–14.

56. Aguilar M, Prieto P. Sequence analysis of wheat subtelomeres reveals a high polymorphism among homoeologous chromosomes. Plant Genome. 2020;13(3):e20065.

57. Zhai H, Jiang C, Zhao Y, Yang S, Li Y, Yan K, et al. Wheat heat tolerance is impaired by heightened deletions in the distal end of 4AL chromosomal arm. Plant Biotechnol J. 2021 May;19(5):1038–51.

58. Sun L, Yang W, Li Y, Shan Q, Ye X, Wang D, et al. A wheat dominant dwarfing line with Rht12 , which reduces stem cell length and affects gibberellic acid synthesis, is a 5AL terminal deletion line. Plant J. 2019;97(5):887–900.

59. Cockram J, Jones H, Leigh FJ, O'Sullivan D, Powell W, Laurie DA, et al. Control of flowering time in temperate cereals: genes, domestication, and sustainable productivity. J Exp Bot. 2007;58(6):1231–44.

60. Guo W, Xin M, Wang Z, Yao Y, Hu Z, Song W, et al. Origin and adaptation to high altitude of Tibetan semi-wild wheat. Nat Commun. 2020;11(1):1–12.

61. Gilmour AR, Cullis BR, Verbyla AP. Accounting for Natural and Extraneous Variation in the Analysis of Field Experiments. J Agric Biol Environ Stat. 1997;2(3):269–93.

62. Shah R. mpMapinteractive: Interactive components for package mpMap. R package version 0.2. 2013.

63. Huang BE, George AW. R/mpMap: A computational platform for the genetic

analysis of multiparent recombinant inbred lines. Bioinformatics. 2011;27(5):727–9.

64. Wilkinson PA, Winfield MO, Barker GLA, Allen AM, Burridge A, Coghill JA, et al. CerealsDB 2.0: an integrated resource for plant breeders and scientists. BMC Bioinformatics. 2012;13(1):219.

65. Paradis E, Schliep K. ape 5.0: an environment for modern phylogenetics and evolutionary analyses in R. Bioinformatics. 2019 Feb 1;35(3):526–8.

66. Winfield MO, Allen AM, Burridge AJ, Barker GLA, Benbow HR, Wilkinson PA, et al. High-density SNP genotyping array for hexaploid wheat and its secondary and tertiary gene pool. Plant Biotechnol J. 2016;14(5):1195–206.

67. Vandesompele J, De Preter K, Pattyn F, Poppe B, Van Roy N, De Paepe A, et al. Accurate normalization of real-time quantitative RT-PCR data by geometric averaging of multiple internal control genes. Genome Biol. 2002;3(7):RESEARCH0034.

68. Zielinski T, Moore AM, Troup E, Halliday KJ, Millar AJ. Strengths and limitations of period estimation methods for circadian data. PLoS One. 2014;9(5).

69. Dakhiya Y, Green RM. Thermal imaging as a non-invasive technique for analyzing circadian rhythms in plants. New Phytol. 2019;224:1685–96.